Land cover classification at three different levels of detail from optical and radar Sentinel SAR data: a case study in Cundinamarca (Colombia)

Juan Ricardo Mancera-Flórez [a] & Ivan Lizarazo [b]

[a] Universidad Nacional de Colombia, sede Bogotá, Facultad de Ciencias Agrarias, Bogotá, Colombia. jrmanceraf@unal.edu.co
[b] Universidad Nacional de Colombia, sede Bogotá, Facultad de Ciencias Agrarias, Grupo de Investigación Análisis Espacial del Territorio y del Cambio Global (AET-CG), Bogotá, Colombia. ializarazos@unal.edu.co

Abstract
In this paper, the potential of Sentinel-1A and Sentinel-2A satellite images for land cover mapping is evaluated at three levels of spatial detail; exploratory, reconnaissance, and semi-detailed. To do so, two different image classification approaches are compared: (i) a traditional pixel-wise approach; and (ii) an object–oriented approach. In both cases, the classification task was conducted using the "RandomForest" algorithm. The case study was also intended to identify a set of radar channels, optical bands, and indices that are relevant for classification. The thematic accuracy of the classifications displays the best results for the object-oriented approach to exploratory and recognition levels. The results show that the integration of multispectral and radar data as explanatory variables for classification provides better results than the use of a single data source.

Keywords: Sentinel-1A; Sentinel-2A; land cover classification; random forest; object-based analysis.

Clasificación de la cobertura del suelo en tres niveles de detalle diferentes a partir de datos ópticos y de radar SAR Sentinel: un estudio de caso en Cundinamarca (Colombia)

Resumen
En este documento, se evalúa el potencial de las imágenes satelitales Sentinel-1A y Sentinel-2A para el mapeo de la cobertura del suelo en tres niveles de detalle; exploratorio, reconocimiento y semi-detallado. Se compara el rendimiento de dos enfoques diferentes de clasificación de imágenes: (i) un enfoque tradicional basado en píxeles; y (ii) un enfoque orientado a objetos. En ambos casos, el proceso de clasificación se realizó utilizando el algoritmo "RandomForest". El estudio también aborda la identificación de un conjunto de canales de radar, bandas ópticas e índices relevantes para la clasificación. La exactitud temática de las clasificaciones, muestra los mejores resultados en el enfoque orientado a objetos para los niveles de exploración y reconocimiento. Los resultados muestran que la integración de datos multiespectrales y de radar como variables explicativas para la clasificación proporciona mejores resultados que el uso de una única fuente de datos.

Palabras clave: Sentinel-1A; Sentinel-2A; clasificación de coberturas; bosques aleatorios; análisis basado en objetos.

1. Introduction

Remote sensing image classification is a digital process that is frequently used to create thematic cartography depicting the terrestrial land surface, as it produces reliable maps of a range of features, at different spatial and temporal scales [1]. Biodiversity, urbanization, agriculture and risk assessment studies, among others, have benefited from remote sensing-based thematic cartography [2,3,4].

Globally, thematic cartography became more important at the end of the 1980s and the years that followed with the inauguration of the European CORINE (Coordination of Information on the Environment) program. This resulted in the definition of the Corine Land Cover (CLC) methodology, a consistent and standardized set of principles, rules and procedures for obtaining thematic information for the European territories. The CLC methodology relies on the interpretation of satellite images, supported by auxiliary information, to classify remotely-sensed data into different categories at different levels of spatial detail. Auxiliary information from field surveys and secondary sources is essential to help identify and confirm the content of certain land cover characteristics that have been detected in the images [5,6,7].

In Colombia, the CLC methodology has been adopted – with minor modifications – as the standard methodology for land cover mapping by Instituto Geográfico Agustín Codazzi (IGAC) and Instituto Colombiano de Estudios Ambientales (IDEAM) [8]. The CLC methodology has been applied in a series of mapping projects at different scales and levels of detail [9].

Remote sensors are usually classified as either active (optical), which depend on sunlight; or passive (radar), which emit their own energy. Of the available information from optical sensors, the Landsat satellite mission data has been the most used by medium-spatial scale projects for land cover mapping, as well as by high spatial scale projects that have used their aerial photographs. Optical sensors have some important limitations, in particular, data collection can be hindered by atmospheric conditions, especially in areas that have cloud cover most of the year [10].

As a way round this, active sensors such as synthetic aperture radar (SAR) instruments can take images of the Earth's surface no matter the atmospheric conditions, and can operate in cloudy conditions and in darkness. Furthermore, SAR images contain data related to surface texture and backscatter properties of land cover and, in the case of sparse vegetation, the upper substrate of the soil [10]. In sum, radar images provide more information than optical images such as the Landsat TM images [11], and their usefulness has been demonstrated by several land cover mapping studies that have used SAR images [12,13,14].

Traditional techniques for the visual interpretation of remotely sensed data, be it radar or optical data, are similar to a certain degree. However, while several studies reveal that for both data types, large amounts of information can be extracted by image interpreters, production of thematic cartography is time intensive, and requires hard work and high-level expertise [15].

The visual interpretation of images for land cover classification is based on the manual delineation of objects and shapes, and the careful observation of spatial features and geometric patterns [7]. Recent advances in software and hardware technologies, especially the design of advanced digital classification techniques, have improved the operational performance of the classification task [16]. However, several authors argue that human interpreters are still key to the land cover mapping process as they possess superior classification capabilities. This explains why digital classification procedures are heavily guided by human interpretation [16,17].

The traditional pixel-based classification techniques, used from 1980 onwards, aim to establish a quantitative and statistical relationship between pixel data and categories of interest (14). Such techniques have limitations when applied to high-spatial resolution images, available since 2000, because they focus on individual pixels which are smaller in size compared to the typical size of the elements being studied, and do not take into account spatial features such as texture, shape and context patterns [14]. Therefore, the pixel-based image analysis approach is very limited when it comes to land cover mapping using high-spatial resolution images, although these limitations can be overcome to some degree if object-based techniques are used [14].

The object-based approach for land cover classification starts by grouping pixels into image-regions, by means of a segmentation task [18] that generates discrete objects or pseudo-polygons, whose size may vary in compliance with several parameters. These include aggregation schemas which may differ depending either on image spatial resolution or the spatial scale of the final map [19].

Gao and Mas [20] compared land cover classification results from the traditional pixel-based technique and the object-oriented method, using different resolutions of SPOT-5 multispectral images. Their results showed that the object-oriented method's thematic accuracy was 25% more accurate than the pixel-based method. Perea et al. [21] used the object-oriented method to carry out the digital classification of an urban-forest area using digital aerial photographs. They obtained a thematic accuracy of 90% and showed that image objects output from the segmentation task may also be used for a further "refined" classification [22].

Random forest is among the most efficient of the different machine learning algorithms for digital classification [23]. A random forest is a collection of hundreds of decision trees that collaborate to produce a reliable classification [23]. The outstanding feature of the random forest technique is that it provides more accurate results than other classification techniques, even when there are more variables than observations [24]. Random forest generalizes the training features well and evaluates the importance of the variables for the classification task [25]. It is also very efficient with large volumes of data [26,27].

This can be seen in the study by Balzter et al. [13], where Sentinel-1 radar images and geomorphometric variables were input into the random forest algorithm for land cover classification. It showed that it is possible to discriminate coverages with a thematic accuracy of up to 68.4%, which is useful for mapping tropical regions with frequent cloud cover. Likewise, Lawrence et al. [28] implemented random forest to discriminate two different invasive plant species, obtaining thematic accuracies of between 66% and 93%, highlighting the potential of random forest for land cover mapping.

The objective of the present study was to compare the accuracy of thematic cartography obtained using two different classification approaches, pixel-based and object-oriented, using the random forest algorithm. In the case study, both Sentinel-1 radar and Sentinel-2 optical images acquired by the European Space Agency (ESA) were used as the main input data. The land cover classifications were obtained in compliance with the CLC methodology adapted for Colombia at three levels of detail: exploratory (Level 1), reconnaissance (Level 2) and semi-detailed (Level 3). The overall aim is to evaluate the potential of Sentinel 1 and Sentinel 2 images for thematic mapping, and hence, to provide empirical evidence to support the work of national mapping agencies which are moving towards digital techniques to replace traditional mapping methods.

2. Materials and methods

2.1. Study Area

The study area is located in the department of Cundinamarca, comprising the municipalities of Facatativá, El Rosal, Madrid, Bojacá, Mosquera and Funza (see Fig. 1). Elevation ranges between 2300 and 2900 masl, with an average height of 2500 meters. Slope varies between 0% and 25% with an average of 18%. The study area covers approx. 30,000 hectares. This area was selected due to the availability of high-quality land cover information, obtained by the Colombian national geographic institute at three different spatial levels, using well-established visual techniques of image analysis.

2.2. Data

2.2.1. Images

The European Space Agency (ESA) Copernicus program is comprised of satellite missions Sentinel 1 and Sentinel 2 [29], offering operational satellite data that is useful for land cover mapping, land change detection and estimation of physical-geochemical variables [30].

Sentinel 1A operates a C-band synthetic aperture radar (SAR) instrument (5.404 GHz) which is not affected by cloud cover or lack of light. The IW (Interferometric Wide) swath mode combines a large scan width (250 km) with a moderate geometric resolution (5 m x 20 m). The IW mode is the most commonly used mode for land cover studies [31].

The Sentinel-1A (Ground Range Detecting) single-level image used was acquired on September 16, 2015. The specifications of the image (Fig. 2) are summarized in Table 1.

Sentinel-2A consists of two polar-orbiting satellites each with a multispectral MSI sensor (Multi Spectral Imager) of high-medium spatial resolution, characterized by a 290-kilometer wide strip and a high revisit capacity (5 days with two satellites) [32].

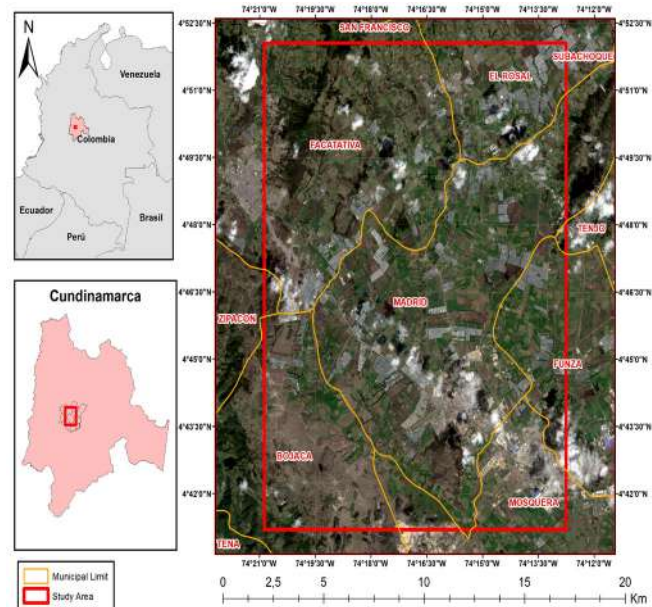The Sentinel-2A MSI images used in this study (Fig. 2) are summarized in Table 2 [31].

Figure 1. Study Area (Image Sentinel 2 A combination of bands 4-3-2)
Source: The Authors.

Table 1.
Specifications of the Sentinel 1A Radar Image. V denotes vertical polarization, H denotes horizontal polarization.

Specifications	Sentinel image - 1A
Acquisition date	September 16 2015
Orbit	Descendant
Image mode	IW
Frequency	Band C (5.4 GHz)
Polarization	VV – VH
Kind of product	Level -1 GRD
Resolution	10 m

Source: The Authors.

Table 2.
Specifications of the Sentinel 2A Optical Image.

| Bands	Spatial resolution (m)	Spectral resolution (nm)	Bandwidth (nm)
Band 1 (Aerosol)	60	443	20
Band 2 (Blue)	10	490	65
Band 3 (Green)	10	560	35
Band 4 (Red)	10	665	30
Band 5 (Near Infrared - NIR)	20	705	15
Band 6 (Near Infrared - NIR)	20	740	15
Band 7 (Near Infrared - NIR)	20	783	20
Band 8 (Near Infrared - NIR)	10	842	115
Band 8a (Near Infrared - NIR)	20	865	20
Band 9 (Water vapor)	60	945	20
Band 10 (Cirrus)	60	1375	30
Band 11 (Short Wave Infrared - SWIR)	20	1610	90
Band 12 (Short Wave Infrared - SWIR)	20	2190	180

Source: The Authors.
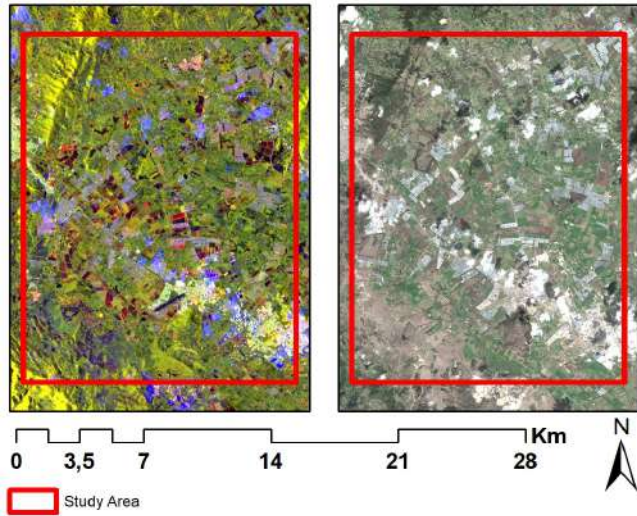
Figure 2. Study Area. Left: Sentinel 1A radar image – polarization combination VV-VH- (VV-VH). Right: Sentinel 2A optical image – color composition RGB 432.
Source: The Authors.

2.2.2. Reference data

The thematic information used as reference for training and validation is a vector data produced by Instituto Geografico Agustin Codazzi (IGAC) and Corporacion Autonoma Regional de Cundinamarca (CAR). The reference dataset comprises thematic cartography in accordance with CLC methodology at scale 1:25,000, semi-detailed level, for the inter-administrative contract CAR-IGAC (1426 / 4705-2016). The reference dataset was obtained using Sentinel-2A images from 2015 and includes land cover classifications from level 1 to level 6, obtained from visual image interpretation conducted by expert cartographers at IGAC.

The CAR reference data for the study area has 41 land cover classes in level 3, 13 land cover classes in level 2, and 5 land cover classes in level 1. For the training step, approximately 10% of the total area for every class was used in order to avoid both over-training and under-training. Then, for the validation step, the remaining 90% of the area was used.

2.3. Methods

The workflow diagram shown in Fig. 3 consists of four stages: in Stage 1, radiometric and geometric corrections were conducted on radar and optical images, and the spectral variables to be analyzed were prepared; in Stage 2, training areas were established in levels 1, 2, 3; in Stage 3, the random forest algorithm was used to classify land cover in the study area, using the pixel and object-oriented techniques and identifying relevant variables to perform the integration of optical and radar data in the classifications for levels 1, 2, 3; in Stage 4, thematic accuracy was assessed for each image analysis technique implemented and for each level of classification.
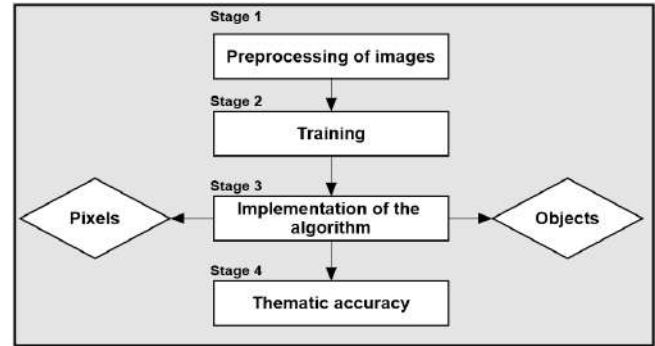

Figure 3. Workflow for this study.
Source: The Authors.

2.3.1. Stage 1. Preprocessing of images

The Sentinel-1A image was calibrated in the Sigma angle of incidence, the multilooking process was applied to two ranges in order to obtain square pixels, the "speckle" or noise was corrected with the Lee Sigma filter in a 5x5 window and topographic distortion was removed using the SRTM 1 arc sec digital elevation model [14]. The digital level (DN) values of the SAR image were converted to backscattering values on the decibel scale (db). All processes were carried out in the SNAP software [14].

The polarimetric data of the Sentinel-1A image (VV - VH) were combined using the method outlined in Abdikan et al. [14], where the most accurate scenario is given using the VV, VH, (VV-VH) polarizations, and (VV / VH) and [(VV + VH) / 2] as training variables for the classification, and four additional combinations were calculated for a total of nine variables.

The variables, obtained from the pre-processing of the polarizations (VV - VH) of the Sentinel-1A radar data and used to carry out the classification of coverages, are shown in Table 3. Here we present the operations and combinations of each variable.

A Sentinel-2A image, obtained on 2015-12-21, was obtained using the Google Earth Engine platform [33]. The data from Sentinel-2A have 13 spectral bands that represent the top-of-atmosphere (TOA) reflectance values, these values were scaled by 10000.

The bands used have resolutions of 10 m and 20 m (B2 - B3 - B4 - B5 - B6 - B7 - B8 - B8a) and were implemented to

Table 3.
Operations and combinations with radar image

Variable	Band	Combination
1	VH	VH
2	VV	VV
3	B1	VV-VH
4	B2	VV/VH
5	B3	(VV+VH)/2
6	B4	VH/VV
7	B5	(VV-VH)/2
8	B6	VV+VH+(VV/VH)
9	B7	VV*VH

Source: The Authors.

calculate the Normalized Difference Vegetation Index (NDVI) [34]. The NDVI index can be used to produce a spectral index that separates the green vegetation from the ground [16]. It is expressed as the difference between the infrared and red bands, normalized by the sum of these bands: as show it in eq. (1).

$$NDVI = \frac{b\ NIR - b\ RED}{b\ NIR + b\ RED} \qquad (1)$$

where b NIR is the infrared band TOA reflectance and b RED is the red band TOA reflectance.

The NDVI values range from -1 to 1, 1 being mature or high-density vegetation and -1 surfaces without vegetation [16].

The Enhanced Vegetation Index (EVI) optimizes the vegetation signal, improving sensitivity in regions of high biomass and reducing atmospheric influences [35]. This index is expressed as shown in eq. (2).

$$EVI = G\ \frac{b\ NIR - b\ RED}{b\ NIR + C_1 * b\ RED - C_2 * b\ BLUE + L} \qquad (2)$$

Where b is band on TOA reflectance, L is the background setting of the canopy that addresses the non-linear differential NIR and the red radiant transfer through a canopy, and $C1$, $C2$ are the coefficients of aerosol resistance, which use the blue band to correct the influence of aerosols in the red band. The coefficients adopted in the EVI algorithm are, $L = 1$, $C1 = 6$, $C2 = 7.5$ and G (gain factor) $= 2.5$ [36,37,35]. Table 4 summarizes all bands and variables implemented from the optical data.

2.3.2. Stage 2. Training

The training areas for the algorithm were extracted from the CAR 1:25000 vector information, at classification levels 1, 2, and 3. We assigned 10% of the area per class for training and the remaining 90% area for validation, as was mentioned in Section 2.2.2.

The supervised classification was implemented using the random forest learning algorithm, which uses an ensemble of decision trees as base classifiers [23]. The trees are constructed from successive binary partitions of the training

Table 4.
Bands and variables with optical image

Bands	Variables
Band 2 (Blue)	B2
Band 3 (Green)	B3
Band 4 (Red)	B4
Band 5 (Near Infrared - NIR)	B5 - NDVI B5 - EVI B5
Band 6 (Near Infrared - NIR)	B6 - NDVI B6 - EVI B6
Band 7 (Near Infrared - NIR)	B7 - NDVI B7 - EVI B7
Band 8 (Near Infrared - NIR)	B8 - NDVI B8 - EVI B8
Band 8a (Near Infrared - NIR)	B8a - NDVI B8a - EVI B8a
TOTAL	18

Source: The Authors.

data set which form subsets of homogeneity [25]. This algorithm requires predictive variables and the number of classification trees be used as input parameters; the value of 500 trees is established by default [27]. Cánovas [38] mentions that using a larger number of trees does not have a significant impact on classification accuracy.

This classification was carried out in the statistical package R using the libraries randomForest, rgdal, rgeos, sp and raster. As stated in Section 2.2.2, the CAR reference data used for the training and validation zones was produced by IGAC in 2016.

2.3.3. Stage 3. Implementation of the algorithm

The random forest algorithm can evaluate predictor variables with two parameters: the average decrease in accuracy (Mean Decrease Accuracy) and the average decrease in Gini (Mean Decrease Gini). The former measures the precision given by a variable in each random tree [25]. The latter measures the homogeneity of the variables in the random trees and is calculated each time an input variable is used to divide a node [27,39].

The classification process was carried out by implementing the random forest algorithm in two phases. In the first phase, the classification was conducted with the three levels of detail in both the pixel and object-oriented approaches, taking the optical and radar data individually. In the second phase, the parameters of (Mean Decrease Accuracy) and the average decrease of Gini (Mean Decrease Gini) were evaluated, in order to identify the best optical and radar variables, and thus, the classification was repeated with the joint data and their accuracy was compared with the individual data.

The pixel approach processing was undertaken in the statistical package R. The object-oriented approach was carried out in the ENVI 5.3 program, from which the segmentation vectors were obtained, and then classified in the statistical package R.

2.3.4. Stage 4. Thematic accuracy Assessment

For assessing thematic accuracy by classification level and by class, a vector layer of point type covering the whole study area was created using a spacing equal to the spatial resolution of the Sentinel-2A radar image (10 m) for a total of 2,699,648 points. This layer carries one attribute that represents visually identified land cover categories for the CAR-IGAC_2016 project as well as the random forest classifications at levels 1, 2, and 3. Confusion matrices were created in order to calculate Kappa indices. This stage was implemented using the *fmsb, psych, foreign* libraries in the statistical package R.

3. Results

3.1. Implementation of the algorithm

The algorithm evaluates the best variables using the aforementioned indices. A frequency graph was prepared (Fig. 4), in which the variables with the best index values for
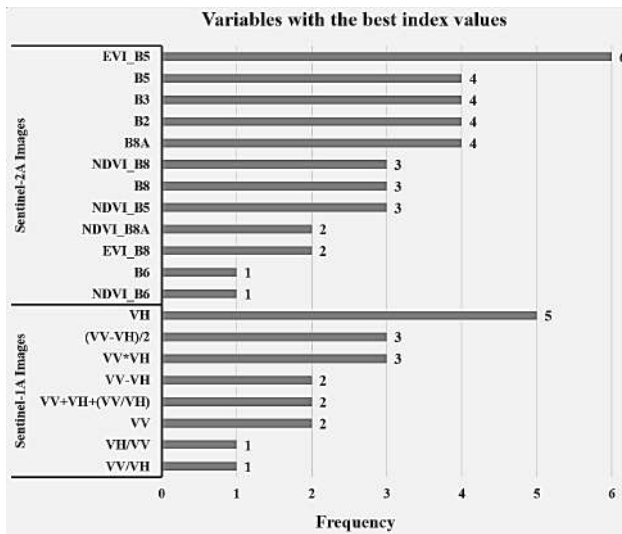
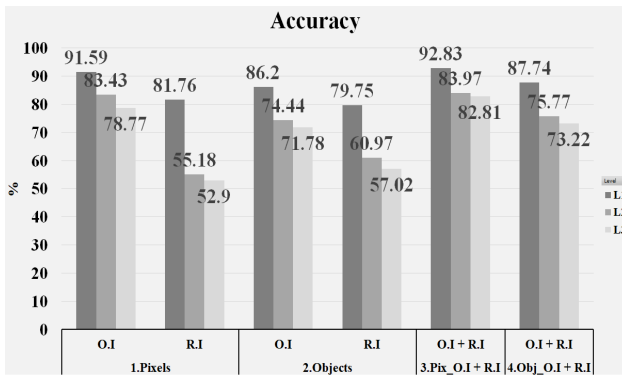Figure 4. Variables with the best index values
Source: The Authors.

Figure 5. Training accuracy for three classification levels, L1, L2, and L3. (O.I = Optical Images, R.I = Radar Images, O.I + R.I = Optical Images with Radar Images.)
Source: The Authors.

optical and radar data in pixel and object-oriented approaches are recorded. 5 variables of the optical data and 3 of the radar data were taken into account, these variables were those that presented the best indices according to the algorithm valuation and these data were integrated into the classifications of the pixel and object-oriented approaches. In this manner, the algorithm's potential as a variable evaluator was measured and the accuracy obtained from the integrated optical and radar data was compared to the data when used individually in each of the implemented approaches.

As shown in Fig. 4, optical and radar data were merged as variables; B2 (Band 2 "Blue"), B3 (Band 3 "Green"), B5 (Band 5 "Near Infrared - NIR"), B8A (Band 8a "Near Infrared - NIR"), EVI_B5 (EVI calculated with Band 5) obtained from the optical data and the variables VH, ("VV - VH" / 2), (VV*VH) corresponding to the radar data.

Fig. 5 shows the results of training accuracy for the two classification approaches at levels 1, 2, and 3.

3.2. Best Classification Variables

The Sentinel-2A sensor channels that improved thematic accuracy were Band 2, Band 3, Band 5, Band 8A, and the variables that were calculated with this sensor. The study identified that the EVI calculated with Band 5 and EVI calculated with the Band 8A contributed more than the other variables and improved the classification.

Of the Sentinel-1A sensor radar data, it was clear that the VH polarization channel was the most suitable for classification, likewise, the variables obtained from this channel that improved accuracy in the resulting classification were the variable calculated from the difference between the VV and VH polarization (VV-VH) and the variable calculated from the mean of the difference between the polarization VV and VH [(VV-VH) / 2].

3.3. Thematic accuracy

The results obtained for thematic accuracy at level 1 are shown in Table 5 and Fig. 6, using the 90% of the CAR dataset, reveal that, firstly, the best global thematic accuracy is obtained from integrated radar and optical images, implementing

Table 5.
Accuracy level 1

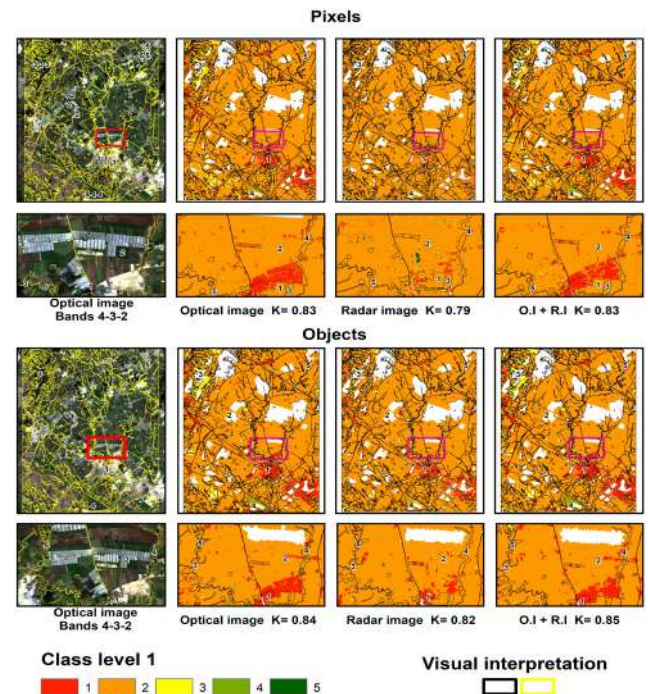| Bands / Variables	Kappa Level 1	
	Pixels	Objects
Optical images	0.83	0.84
Radar images	0.79	0.82
Optical + Radar Images	0.83	0.85

Source: The Authors.

Figure 6. Thematic Accuracy for level 1. (O.I + R.I = Optical Images with radar images.)
Source: The Authors.

the object-oriented approach resulting in a kappa index of K = 0.85. Secondly, we observed that the object-oriented approach applied to optical images presents with K = 0.84. Thirdly, it was found that the pixel-based approach from both optical images and integrated optical and radar images share the same accuracy at K = 0.83.

The results obtained from the classification at level 2 are shown in Table 6 and Fig. 7. These results reveal that the best global thematic accuracies are obtained from, firstly, the implementation of the integrated radar and optical images using the object-oriented approach, resulting in K = 0.62. Secondly, the pixel approach which used the integrated optical and radar images together with the object-oriented approach using optical images resulted in K = 0.60. Thirdly, the pixel approach using optical images produced K = 0.59. The remaining classifications obtained from the object-oriented approach with radar and pixel images show lower kappa indexes, K = 0.57 and K = 0.49 respectively.

The results obtained from the classification for Level 3 are shown in Table 7 and Fig. 8. The combinations that demonstrated the best global thematic accuracies were, in first place, the integration of radar and optical images using an object-oriented approach resulting in K = 0.60. In second, the use of a pixel approach with optical images produced K = 0.58. In third place, the pixel approach applied to integrated optical and radar images gave K = 0.57. Fourth, applying the object-oriented approach to radar images and the pixel approach to optical images both resulted in K = 0.56. Finally, the pixel-wise approach with radar images produced K = 0.47.
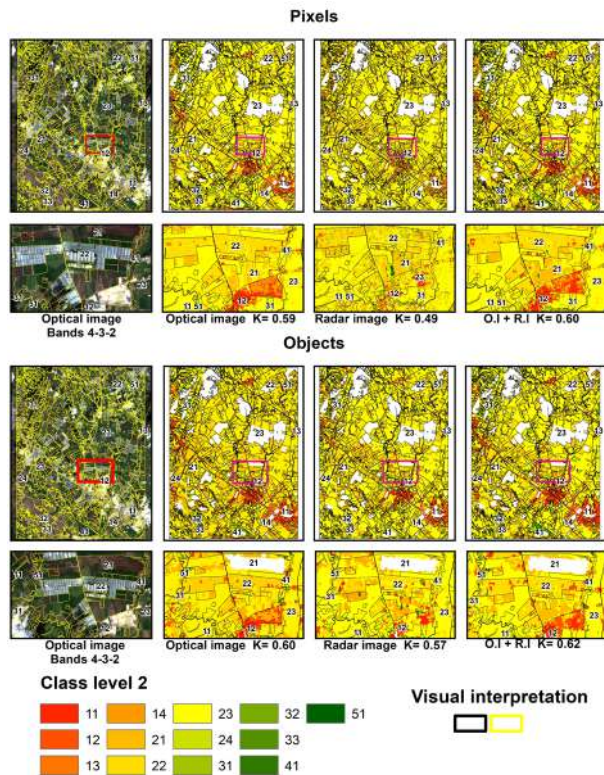
Table 6.
Accuracy level 2

Bands / Variables	Kappa Level 2	
	Pixels	Objects
Optical images	0.59	0.6
Radar images	0.49	0.57
Optical + Radar Images	0.6	0.62

Source: The Authors.

Table 7.
Accuracy level 3

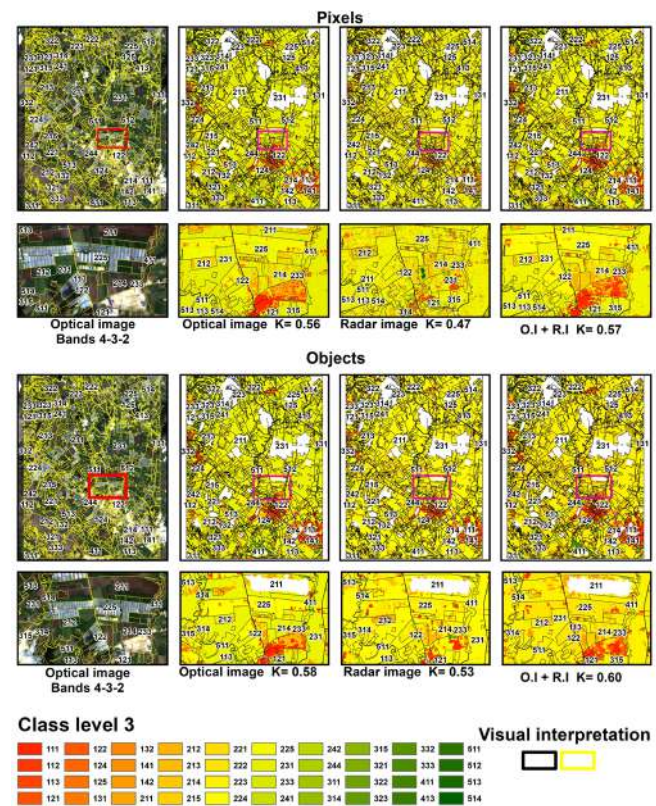| Bands / Variables	Kappa Level 3	
	Pixels	Objects
Optical images	0.56	0.58
Radar images	0.47	0.53
Optical + Radar Images	0.57	0.6

Source: The Authors.

Figure 8. Thematic Accuracy for level 3. (O.I + R.I = Integrated Optical and Radar Images.)
Source: The Authors.

4. Discussion

From the thematic accuracy values shown in Fig. 9, it is evident that the most informative variables are obtained from the integration of optical and radar data. Overall thematic accuracy is higher when both the pixel-based and the object-oriented approaches are applied to integrated images rather than the optical or radar datasets by themselves. The model's accuracy when integrated data is used is approximately 10% higher than with the single datasets.

Figure 7. Thematic Accuracy for level 2. (O.I + R.I = Integration optical and radar images.)
Source: The Authors.

The most relevant variables were: B3 (Band 3 "Green"), B5 (Band 5 "Near Infrared - NIR"), EVI_B5 (EVI calculated with Band 5) obtained from the optical data and the variables VH, ("VV - VH" / 2), (VV*VH) corresponding to the radar data. This set of variables confirm results previously obtained by Balzter [13] and Abdikan [14]. They claim that the combination of radar data with other types of variables or data can lead to greater accuracy in the classifications. The results of this study ratify the potential of RandomForest as a classification algorithm and its ability to evaluate the importance of explanatory variables [40,23].

Regarding the best approach for thematic accuracy of land cover classification, here the object-oriented technique was superior to the traditional pixel-based technique by approx. 5%, as shown in Fig. 9. This shows that the classifications obtained by applying the object-oriented technique produces higher thematic accuracy than traditional per-pixel methods [41,42,43,44].

In this study, the volume of processed data was huge, as it combined the optical data and the radar data (20 Gigabytes). Thus, it was a suitable scenario to test the high-level processing capacity of the random forest machine learning algorithm. Our results reaffirm the suitability of this algorithm for image classification, as was suggested by Balzter [13] and Abdikan [14].

The results of the classification for level 1 confirm the findings of Vargas [45,46], indicating that, for exploratory detail level where land cover is mapped on a scale of 1: 100,000, Kappa indices greater than K = 0.81 are outstanding classifications (Fig. 10).

At level 2, i.e., mapping at reconnaissance level at a scale of 1:50,000 to 1:25,000, in general, the best results were obtained by integrating radar and optical images using the object-oriented approach. Thematic accuracy corresponding to Kappa = 0.62 represents an acceptable quality (Fig. 10).

At level 3, for mapping studies at a semi-detailed level, corresponding to scales of 1:25,000 to 1:10,000, the best results were obtained with the combination of optical and radar images using an object-oriented approach. Thematic accuracy with Kappa = 0.62 represents moderate quality (Fig. 10).
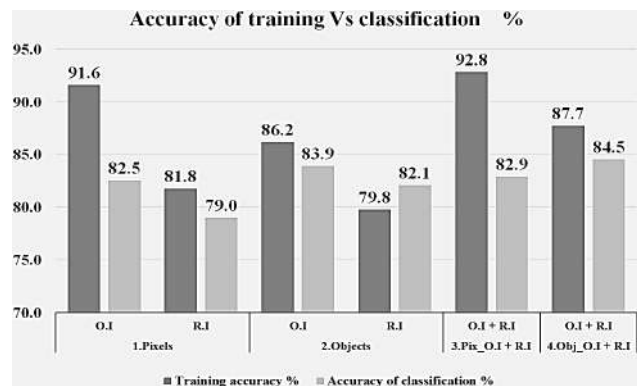

Figure 9. Thematic accuracy vs. Training (O.I = Optical Images, R.I = Radar Images, O.I + R.I = Optical Images with Radar Images.)
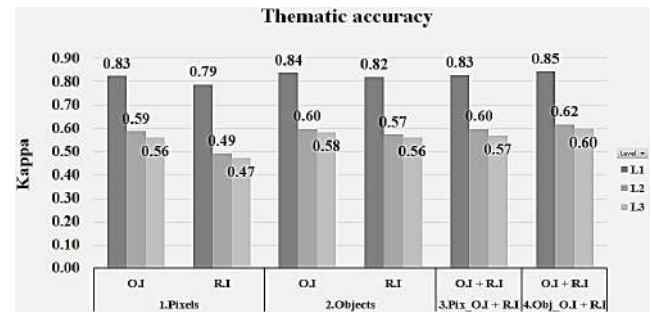Source: The Authors.

Figure 10. Thematic accuracy for level. (O.I = Optical Images, R.I=Radar Images, O.I + R.I = Optical Images with Radar Images.)
Source: The Authors.

5. Conclusions

This study ascertained the performance of digital classification techniques for land cover classification. Sentinel-1 A optical data and Sentinel-2 radar data were used, both individually and in combination, for discrimination of land cover. Two different image analysis techniques, the pixel-based and object-oriented approaches, as well as the random forest algorithm, were applied to obtain land cover classes at three different spatial scales as specified by the Corine Land Cover methodology.

We obtained the best accuracy at level 1, combining optical and radar data with the object-oriented approach, and obtaining Kappa indexes greater than 0.80. This showed that the combination of optical and radar data with object-oriented classification is ideal for the identification of land cover at level 1.

Thematic accuracies decrease by an average of 19% as the level of detail and classes increases, with the "exploratory" level 1 presenting the best results for thematic mapping using the techniques, data and methods presented in this work. The thematic accuracies obtained using the object-oriented approach are superior to the pixel-based approach by 5%. In addition, it was shown that the integration of radar and optical images improves the quality of land cover mapping. To conclude, the results of this study show the potential and the limitations of using available optical and radar satellite data, as well as different digital image analysis techniques, for land cover classification at several spatial scales.

References

[1] Giles-M .F., Status of land cover classification accuracy assessment. Remote Sensing of Environment 80(1), pp. 185-201, 2002. DOI: 10.1016/S0034-4257(01)00295-4

[2] Ullmann, T., Schmitt, A., Roth, A., Duffe, J., Dech, S., Hubberten, H. W. and Baumhauer, R., Land cover characterization and classification of arctic tundra environments by means of polarized synthetic aperture X-and C-Band Radar (PolSAR) and Landsat 8, 2014. DOI: 10.3390/rs6098565

[3] Falcucci, A., Maiorano, L. and Boitani, L., Changes in land-use/land-cover patterns in Italy and their implications for biodiversity conservation. Landscape ecology, 22(4), pp. 617-631, 2007. DOI: 10.1007/s10980-006-9056-4

[4] Van der Sande, C.J., de Jong, S.M. and de Roo, A.P.J., A segmentation and classification approach of IKONOS-2 imagery for land cover mapping to assist flood risk and flood damage assessment, International Journal of Applied Earth Observation and Geoinformation, 4(3), pp. 217-229, 2003. DOI: 10.1016/S0303-2434(03)00003-5

[5] Heymann, Y., Steenmans, C., Croisille, G. and Bossard, M., Corine land cover project-technical guide. European Commission, Directorate General Environment. Nuclear safety and civil protection, ECSC-EEC-EAEC, Brussels-Luxembourg, 1994, 136 P.

[6] Bossard, M., Feranec, J. and Otahel, J., Corine land cover technical guide: Addendum, 2000.

[7] Bussay, A., Tóth, T., Juškevičius, V. and Seguini, L., Evaluation of aridity indices using SPOT normalized difference vegetation index values calculated over different time frames on Iberian rain-fed arable land. Arid Land Research and Management, 26(4), pp. 271-284, 2012. DOI: 10.1080/15324982.2012.694398

[8] IDEAM, IGAC y CORMAGDALENA., Mapa de cobertura de la tierra Cuenca Magdalena-Cauca: metodología CORINE Land Cover adaptada para Colombia a escala 1:100.000. Instituto de Hidrología, Meteorología y Estudios Ambientales, Instituto Geográfico Agustín Codazzi y Corporación Autónoma Regional del río Grande de La Magdalena. Bogotá, D.C., 2008, 200 P. + 164 hojas cartográficas.

[9] IGAC y CORPORACION AUTONOMA REGIONAL DEL QUINDIO. Instituto Geográfico Agustín Codazzi. Coberturas y usos de la tierra del Departamento del Quindío Escala 1:10000. 2010.

[10] Guzmán, I.D.G., Posada, E., Duarte, L.P.A. and García, J.E., Descripción del programa de investigación en desarrollo satelital y aplicaciones en el tema de observación de la tierra. Comisión Colombiana del Espacio–CCE Grupo de Observación de la Tierra, 4, 2010.

[11] Beaulieu, N., Hill, P., Leclerc, G. y Escobar, G., Cartografía de la cobertura de la tierra en el municipio de Puerto López, Colombia, utilizando imágenes de RADARSAT-1 y de JERS-1. En Memoria del Simposio final GlobeSAR, Vol. 2, 1999, pp. 17-20.

[12] Niu, X. and Ban, Y., Multi-temporal RADARSAT-2 polarimetric SAR data for urban land-cover classification using an object-based support vector machine and a rule-based approach. International Journal of Remote Sensing, 34(1), pp. 1-26, 2013. DOI: 10.1080/01431161.2012.700133

[13] Balzter, H., Cole, B., Thiel, C. and Schmullius, C., Mapping CORINE land cover from Sentinel-1A SAR and SRTM digital elevation model data using Random Forests. Remote Sensing, 7(11), pp. 14876-14898, 2015. DOI: 10.3390/rs71114876

[14] Abdikan, S., Sanli, F.B., Ustuner, M. and Calò, F., Land cover mapping using SENTINEL-1 SAR data. ISPRS-International Archives of the Photogrammetry, Remote Sensing and Spatial Information Sciences, 2016, pp. 757-761. DOI: 10.5194/isprsarchives-XLI-B7-757-2016

[15] Addink, E.A., Van Coillie, F.M. and De Jong, S.M., Introduction to the GEOBIA 2010 special issue: from pixels to geographic objects in remote sensing image analysis. International Journal of Applied Earth Observation and Geoinformation, 15, pp. 1-6, 2012. DOI: 10.1016/j.jag.2011.12.001

[16] Eastman, J.R. IDRISI Selva manual. Clark University. Worcester, Massachusetts, USA, [online]. 2012. Available at: https://scholar.google.com/scholar_lookup?title=IDRISI+Selva+Manual&author=Eastman,+J.R.&publication_year=2012

[17] Hay, G.J. and Castilla, G., Geographic object-based image analysis (GEOBIA): a new name for a new discipline. In: Object-based image analysis. Springer, Berlin Heidelberg, 2008, pp. 75-89. DOI: 10.1007/978-3-540-77058-9_4

[18] Lizarazo, I. and Elsner, P., Fuzzy regions for handling uncertainty in remote sensing image segmentation. In: International Conference on Computational Science and Its Applications. Springer, Berlin, Heidelberg, 2008, pp. 724-739. DOI: 10.1007/978-3-540-69839-5_53

[19] UEGPS. Metodología para clasificación de coberturas a partir del procesamiento de imágenes satelitales. Unidad Ejecutora Gestión de Proyectos Sectoriales. Ministerio de Agricultura y Riego. Lima-Perú, 2018.

[20] Gao, Y and Jf Mas., A comparison of the performance of pixel based and object based classifications over images with various spatial resolutions. Online Journal of Earth Sciences 2(8701), pp. 27-35, 2008.

[21] Perea, A.J., Meroño, J.E. and Aguilera, M.J., Object-based classification in aereal digital photography for land-use discrimination. Interciencia, 34(9), pp. 612-616, 2009.

[22] Rodríguez, A., Metodología para detectar cambios en el uso de la tierra utilizando los principios de la clasificación orientada a objetos, estudio de caso piedemonte de Villavicencio, Meta, Tesis de Maestría. Facultad de Ingeniería Agronómica. Universidad Nacional de Colombia, Bogotá D.C., Colombia, 2011.

[23] Breiman, L., Random forests. Machine learning, 45(1), pp. 5-32, 2001. DOI: 10.1023/A:1010933404324

[24] Pal, M., Random forest classifier for remote sensing classification. International Journal of Remote Sensing, 26(1), pp. 217-222, 2005. DOI: 10.1080/01431160412331269698

[25] Prasad, A.M., Iverson, L.R. and Liaw, A., Newer classification and regression tree techniques: bagging and random forests for ecological prediction. Ecosystems, 9, pp. 181-199, 2006. DOI: 10.1007/s10021-005-0054-1

[26] Urrea-Gales, V., Detección de interacciones genéticas asociadas a enfermedades complejas. Aplicación al cáncer de vejiga. Tesis de Maestría. Departamento de Estadística en Investigación Operativa Universidad Politécnica de Cataluña, Barcelona, España, 2009.

[27] Liaw, A. and Wiener, M., Classification and regression by Random Forest. R news, 2(3), pp. 18-22, 2002.

[28] Lawrence, R.L., Wood, S.D. and Sheley, R.L., Mapping invasive plants using hyperspectral imagery and Breiman Cutler classifications (RandomForest). Remote Sensing of Environment, 100(3), pp. 356-362, 2006. DOI: 10.1016/j.rse.2005.10.014

[29] Van der Meer, F.D., Van der Werff, H.M.A. and Van Ruitenbeek, F.J.A., Potential of ESA's Sentinel-2 for geological applications. Remote Sensing of Environment, 148, pp. 124-133, 2014. DOI: 10.1016/j.rse.2014.03.022

[30] Drusch, M., Del Bello, U., Carlier, S., Colin, O., Fernandez, V., Gascon, F. and Meygret, A., Sentinel-2: ESA's optical high-resolution mission for GMES operational services. Remote Sensing of Environment, 120, pp. 25-36, 2012. DOI: 10.1016/j.rse.2011.11.026

[31] ESA. Sentinel-1 User Handbook, September 2013: ESA User Guide, GMES-S1OP-EOPG-TN-13-0001. European Space Agency, Paris, France, 2013, 80 P.

[32] Mbulisi, S, Mutanga, O. and Rouget M., Examining the potential of Sentinel-2 MSI spectral resolution in quantifying above ground biomass across different fertilizer treatments. ISPRS Journal of Photogrammetry and Remote Sensing 110, pp. 55-65, 2015. DOI: 10.1016/j.isprsjprs.2015.10.005

[33] Gorelick, N., Hancher, M., Dixon, M., Ilyushchenko, S., Thau, D. and Moore, R., Google Earth Engine: planetary-scale geospatial analysis for everyone. Remote Sensing of Environment, 202, pp. 18-27, 2017. DOI: 10.1016/j.rse.2017.06.031

[34] Rouse, J.W. Jr., Haas, R.H., Deering, D.W., Schell, J.A., and Harlan, J.C., Monitoring the vernal advancement and retrogradation (green wave effect) of natural vegetation. NASA/GSFC Type III Final Report, Greenbelt, MD., 1974, 371 P.

[35] Huete, A., Didan, K., Miura, T., Rodriguez, E.P., Gao, X. and Ferreira, L.G., Overview of the radiometric and biophysical performance of the MODIS vegetation indices. Remote Sensing of Environment, 83(1-2), pp. 195-213, 2002. DOI: 10.1016/S0034-4257(02)00096-2

[36] Huete, A., Justice, C. and Liu, H., Development of vegetation and soil indices for MODIS-EOS. Remote Sensing of Environment, 49(3), pp. 224-234, 1994. DOI: 10.1016/0034-4257(94)90018-3

[37] Huete, A.R., Liu, H.Q., Batchily, K.V. and Van Leeuwen, W.J.D.A., A comparison of vegetation indices over a global set of TM images for EOS-MODIS. Remote Sensing of Environment, 59(3), pp. 440-451, 1997. DOI: 10.1016/S0034-4257(96)00112-5

[38] Cánovas-García, F., Análisis de imágenes basado en objetos (OBIA) y aprendizaje automático para la obtención de mapas de coberturas del suelo a partir de imágenes de muy alta resolución espacial: aplicación en la Unidad de Demanda Agraria nº 28, cabecera del Argos. Tesis Dr. Departamento de Geografía. Universidad de Murcia. Murcia, España. 2012.

[39] Breiman, L., Random Forest: Breiman and Cutler's Random Forests for classification and regression. R package version 4.6-12, 2006. Software available at URL: https://cran. rproject. org/web/packages/randomForest

[40] Gounaridis, D. and Koukoulas, S., Urban land cover thematic disaggregation, employing datasets from multiple sources and Random Forests modeling. International Journal of Applied Earth Observation and Geoinformation, 51, pp. 1-10, 2016. DOI: 10.1016/j.jag.2016.04.002

[41] Lizarazo, I. and Elsner, P., Segmentation of remotely sensed imagery: moving from sharp objects to fuzzy regions. Image Segmentation, 2011. DOI: 10.5772/15421

[42] Blaschke, T., Burnett, C. and Pekkarinen, A., Image segmentation methods for object-based analysis and classification, in: de Jong, S. and van derMeer, F. (eds), Remote sensing image analysis: including the spatial domain, Springer, 2006, pp. 211-236. DOI: 10.1007/1-4020-2560-2_12

[43] Lang, S., Albretch, F. and Blaschke, T., Tutorial: introduction to object-based image analysis, Centre for Geoinformatics - Z-GIS, 2006.

[44] Platt, R.V. and Rapoza, L., An evaluation of an object-oriented paradigm for land use/land cover classification, The Professional Geographer 60(1), pp. 87-100, 2008. DOI: 10.1080/00330120701724152

[45] Vargas-Ulate, G., Cartografía fitogeográfica de la Reserva Biológica de Carara, San José, Costa Rica. Editorial de la Universidad de Costa Rica, 1992, 49 P.

[46] Cerda, J. y Villarroel, L., Evaluación de la concordancia inter-observador en investigación pediátrica: coeficiente de Kappa. Revista Chilena de Pediatría, 79(1), pp. 54-58, 2008. DOI: 10.4067/S0370-41062008000100008

J.R. Mancera-Florez, received the BSc. Eng in Forestry in 2014 from the Universidad Distrital Francisco José de Caldas, Bogotá, Colombia, MSc. in Geomatics in 2019 from the Universidad Nacional de Colombia. From 2018 to 2019, he worked for the Instituto Geográfico Agustín Codazzi, Colombia. His research interests focus on remote sensing and its application to the monitoring and study of land cover.
ORCID: 0000-0003-1321-1424

I. Lizarazo, received the BSc. Eng in Civil Engineering in 1981, MSc. in Geographic Information Science in 2004, and PhD in Geography in 2011. From 1992 to 1998, he worked for the Instituto Geográfico Agustín Codazzi, Colombia, and since 1999 he works as Professor for Geoinformatics, first for the Universidad Distrital Francisco José de Caldas, Colombia and later, since 2016, for the Universidad Nacional de Colombia. His research interests focus on the application of machine learning & deep learning techniques to realize the potential of Earth observations and geospatial information to advance the 2030 Agenda for Sustainable Development.
ORCID: 0000-0002-9954-6921